Astron. Astrophys. 350, 541–552 (1999)

ASTRONOMY AND ASTROPHYSICS

The circumstellar environment of UX Ori⋆

A. Natta[1], **T. Prusti**[2], **R. Neri**[3], **W.F. Thi**[4], **V.P. Grinin**[5,6], **and V. Mannings**[7]

[1] Osservatorio Astrofisico di Arcetri, Largo E.Fermi 5, 50125 Firenze, Italy
[2] ISO Data Centre, Astrophysics Division, Space Science Department of ESA, Villafranca del Castillo, P.O. Box 50727, 28020 Madrid, Spain
[3] IRAM, 300 Rue de la Piscine, Domaine Universitaire, 38406 St. Martin d'Hères Cedex, France
[4] Leiden Observatory, P.O. Box 9513, 2300 RA Leiden, The Netherlands
[5] Crimean Astrophysical Observatory, Crimea, 334413 Nauchny, Ukraine
[6] St. Petersburgh University, 198904 St. Petersburgh, Russia
[7] JPL, California Institute of Technology, MS 169–327, 4800 Oak Grove Drive, Pasadena, CA 91109, USA

Received 7 June 1999 / Accepted 30 July 1999

Abstract. This paper presents new observations of UX Ori obtained with the millimeter interferometer of Plateau de Bure and with ISO. UX Ori is the prototype of a group of pre-main–sequence, intermediate-mass stars, often indicated as precursors of β Pic. The interferometry observations at 1.2 and 2.6 mm show that UX Ori has a circumstellar disk, with outer radius $\lesssim$100 AU. We determine the spectral index between these two wavelengths to be 2.1±0.2, consistent with the disk being optically thick at mm wavelengths. Alternatively, the disk solid matter can be in the form of "pebbles" (radius∼10 cm). In both cases most of the disk mass must be in gas form, and small grains must be present, at least in the disk atmosphere. In both cases also, the disk must be rather massive ($\gtrsim 0.1\,M_\odot$). The existence of a circumstellar disk supports the model of the UXOR phenomenon in terms of a star+disk system. Self-consistent models of almost edge-on disks account well for the observed emission at all wavelengths longer than about 8μm, if we include the emission of the optically thin, superheated layers that enshroud the disk. These rather simple disk models fail to account for the strong emission observed in the near-IR (i.e., between ~ 2 and 7 μm), and we suggest a number of possible explanations.

Key words: stars: circumstellar matter – stars: formation – stars: individual: UX Ori

1. Introduction

UX Ori is a Herbig Ae/Be (HAe/Be) star, i.e., a pre-main–sequence star of intermediate mass, located at a distance of about 430 pc. It has spectral type A3, mass $M_\star \sim 2.5\,M_\odot$, and age $\sim 2\times10^6$ yr, based on its location on the HR diagram. The star is optically visible, with an estimated extinction of 0.3–0.5 mag in the visual. UX Ori has a strong IR excess, interpreted by Hillenbrand et al. (1992) as due to a circumstellar disk, similar to those associated with T Tauri Stars (TTS). A brief discussion of the stellar parameters, which are reported in Table 1, is given in Appendix A. The main interest in UX Ori lies in its complex spectrometric, photometric and polarimetric variability, which has now been monitored for many years. The star is strongly variable in the visual, with sporadic deep minima (more than 2 mag in V) occurring roughly with a frequency of 1–2 per year, with a duration of a few days (Bibo & Thé 1990, 1991). During these minima, the stellar light first becomes redder, then bluer again. At the same time, the fraction of polarized light increases to values of few percent (Voshchinnikov et al. 1988). The current interpretation is that UX Ori is surrounded by a circumstellar flattened cloud of relatively small particles (often referred to as a disk), that scatters and polarizes a fraction of the stellar light (Grinin 1988; Grinin et al. 1991). Normally, this is only a small fraction of the total radiation received by the observer. The system contains also dense condensations of dust ("clumps"), which occasionally occult the star and cause the deep minima. At that point, the fraction of stellar radiation received directly drops, while the fraction seen after being scattered by the disk remains practically unchanged and represents a significant contribution to the total. Estimates of the mass of dust in such clumps are of the order of $10^{20}-10^{21}$ g (Voshchinnikov & Grinin 1991; Meeus et al. 1998), similar to the largest comets in the Solar system. A necessary condition of these models is that the disk is seen almost edge-on ($\theta > 70\,\mathrm{deg}$; Voshchinnikov et al. 1988).

The line spectrum of UX Ori is rich in circumstellar lines typical of all pre-main–sequence stars. Some of these lines, in particular lines of low-ionization metals, show sporadic, highly red-shifted absorption components. The presence of infalling gas in the vicinity of the star ($\lesssim 10\,R_\star$; Grinin et al. 1994) has been interpreted as due to the evaporation of large solid bodies (planetesimals or protocomets), in star-grazing orbits around the star (Grady et al. 2000). According to this interpretation, UX Ori is a precursor of β Pic systems.

UX Ori is not an isolated case; it is in fact the prototype of a quite large group of pre-main–sequence stars of similar

Send offprint requests to: natta@arcetri.astro.it

⋆ Based in part on observations obtained with ISO. ISO is an ESA project with instruments funded by ESA Member States (especially the PI countries: France, Germany, the Netherlands and the United Kingdom) and with the participation of ISAS and NASA.

Table 1. UX Ori Parameters

D	430 pc
ST	A3
$T_\star$	8600 K
$L_\star$	48 $L_\odot$
$R_\star$	2.2×10^{11} cm
$M_\star$	2.5 $M_\odot$
Age	2×10^6 yr
A_V	0.5 mag
θ	$\gtrsim$70 deg

mass, called UXORs (after Herbst et al. 1994), which show very similar phenomena. UXORs may provide the best sample of stars to investigate the earliest stages of planet formation, where one can see observational evidence of disk evolution. However, efforts in this direction have not provided conclusive results (Natta et al. 1997). In fact, the evidence for a circumstellar disk around UX Ori follows only from the interpretation of the visual variability described above.

This paper presents a new set of observations of the infrared and millimeter spectrum of UX Ori, which include interferometric observations of the continuum emission at 1.2 and 2.6 mm, a re-analysis of IRAS data at 60 and 100 μm, and a set of ISO observations: PHOT broad-band photometry over the wavelength range 3.6–200 μm, PHOT-S low-resolution spectra in the interval 2.5–11.6 μm and SWS high-resolution observations in some selected intervals in the mid-infrared. We propose an interpretation of these observations in terms of a rather massive circumstellar disk enshrouded by an optically thin, hotter atmosphere (Calvet et al. 1991; Chiang & Goldreich 1997 (CG97); D'Alessio et al. 1998). This interpretation allows us to account for most of the observed properties of UX Ori itself, and may be relevant to further studies of the UXOR phenomenon in general.

2. Observations and results

2.1. Millimeter interferometry

Observations of UX Ori were made simultaneously at 2.6 mm and 1.2 mm in the interferometer's (IRAM, Plateau de Bure – France) standard BC set of 5-antenna configurations on January 25 and March 2, 1998. Visibilities were obtained in both C and D configurations of the array, yielding projected baselines which range from about 280 m down to the antenna diameter of 15 m. The $44''$ ($20''$ at 1.2 mm) primary beam field of the interferometer was centered at α_{J2000} =05:04:30.0 and $\delta_{J2000} = -$03:47:14.0.

At 1.2 mm, data were taken in double sideband mode with the receivers tuned to 240 GHz. The spectral correlator covered an effective bandwidth of 420 MHz, equivalent to a velocity range of 520 km/s. At 2.6 mm, observations were made in upper sideband only, with the SIS receivers tuned to 110.201 GHz. The spectral correlator covered a continuum bandwidth of 280 MHz with a 20 MHz high resolution unit centered at the rest frequency of the ^{13}CO($J = 1 - 0$) transition providing a nominal spectral resolution of 78 KHz, or equivalently 210 m S^{-1} at this frequency.

Visibilities were obtained using on-source integration times of 20 minutes interspersed with 4 minutes calibration on 0458–020. The atmospheric phase noise on the most extended baselines ranged between 5° and 20° at 2.6 mm (20° and 40° at 1.2 mm), consistent with seeing conditions ($0.4'' - 0.8''$) typical for winter weather conditions. The absolute flux density scale which was established on the basis of cross-correlations on 3C273 and on the radio continuum of the post-AGB star CRL 618 (1.8 Jy at 2.6 mm, 2.0 Jy at 1.2 mm), is in full agreement with the interferometric efficiency and should be accurate to 10% at 2.6 mm and to better than 20% at 1.2 mm. The receiver passband shape was determined on 3C273 and was better than 5% throughout the observations.

Data calibration was performed in the antenna-based manner. Cleaned maps were obtained from the visibilities using the standard IRAM deconvolution procedures. The synthesized beam, as determined by fitting a Gaussian to the dirty beam, was found to be $2.1'' \times 0.7''$ at 1.2 mm and $3.8'' \times 1.4''$ at 2.6 mm and is oriented north-south. Due to the low declination of the source, the uv-coverage is unevenly sampled with a maximum spacing of 150 m in the north-south direction and of 280 m east-west. The corresponding east-west linear scale at the distance of the source for an assumed distance $D = 430$ pc is 300 AU at 1.2 mm. At 1.2 mm, we derived a one σ continuum point source sensitivity limit of 1 mJy/beam corresponding to an rms brightness temperature of 13.6 mK, fully consistent with a total on-source integration time of 10 hours and a mean system temperature of 350 K. At 2.6 mm, we obtained a continuum sensitivity limit of 360 μJy/beam, equivalent to an rms brightness temperature of 7 mK.

A continuum source was detected at 1.2 mm and 2.6 mm close to the position of the array's phase tracking center (see Table 2). The source was well-detected on all the baselines and shows a size smaller than $0.5''$. The source is likely to be point-like, the gaussian model fitted to the visibility profile at 1.2 mm being fully consistent with the signal-to-noise level, and the atmospheric seeing.

2.2. IRAS

The raw IRAS data at 60 and 100 μm were re-analyzed in view of the moderate flux quality flag in the Point Source Catalog at 100 μm. As expected, the 60 μm data showed a clear point source at the position of UX Ori. At 100 μm there was indication of complex structure and we constructed high resolution images by using maximum entropy techniques by Bontekoe et al. (1994). For reference we produced also a similar high resolution image for 60 μm. These HIRAS images cover an area of 32 by 32 arcmin with 15 arcsec pixel size.

The HIRAS image at 60 μm shows a clear point source at the position of UX Ori (Fig. 1). This is consistent with the good quality flag of the 60 μm flux in the Point Source Catalog. As expected, the 100 μm HIRAS image shows more complex structure (Fig. 2). Instead of a point source there is a clumpy struc-

Table 2. Millimeter interferometric observations

	1.2 mm		2.6 mm	
Position (J2000)	05:04:30.00	−03:47:14.3	05:04:30.00	−03:47:14.7
Flux density S (mJy)	19.8±2.0		3.8±0.4	

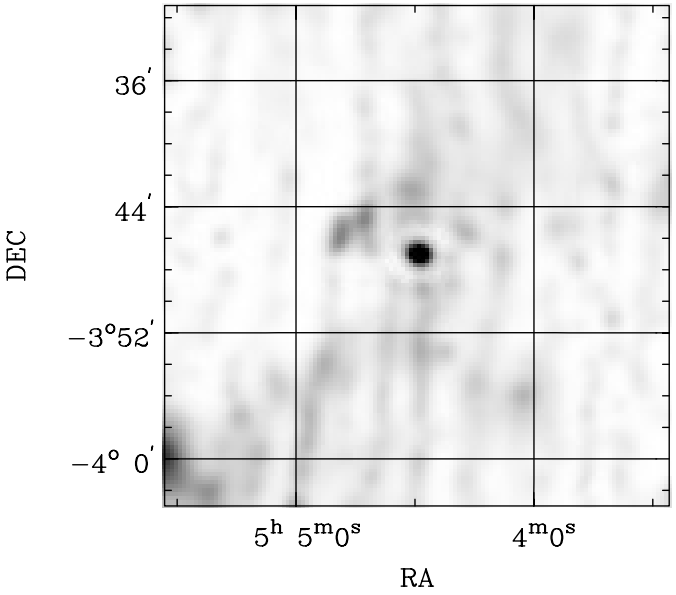

Fig. 1. High resolution 60 μm IRAS image of the region around UX Ori

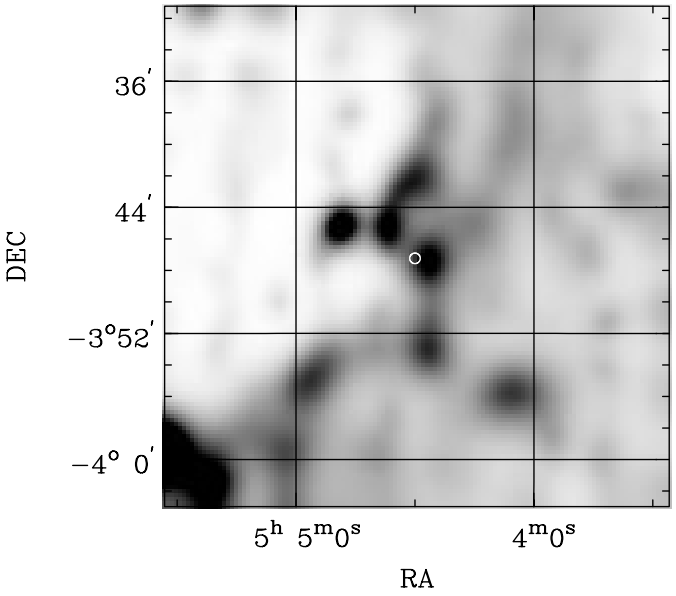

Fig. 2. High resolution 100 μm IRAS image of the region around UX Ori. The location of the star is marked with a circle

ture around the star. UX Ori is located on a ridge between two clumps. In addition there is a new point like 100 μm source at $\alpha_{\rm J2000} = 05$:04:48.0 and $\delta_{\rm J2000} = -03$:45:14. There are no known sources close to this position. The clumps are likely to be part of an interstellar cloud in the vicinity of UX Ori, but this cannot be verified without additional observations.

Due to the clumps and the extended emission, the background emission around UX Ori is variable in the surroundings of the star. In order to interpret the ISO data it is important to note that the 100 μm emission is strongest towards NE and W. Towards N the emission is lower and the lowest background emission is in the SE direction.

2.3. ISO-PHOT

The ISOPHOT observations were obtained March 22, 1998. The photometric measurements of UX Ori were part of an ISO programme aimed at studying the circumstellar environment of UXORs. The sequence contained a spectrophotometric measurement, a background photometric measurement two arc minutes off target, a photometric measurement and small maps at 150 and 200 μm. The spectrophotometric measurement was done with 256 s integration time in the wavelength ranges 2.5–4.8 and 5.8–11.6 μm with resolving power of about 90. The off measurement was done with 32 s integration time per filter at 3.6, 7.3, 12, 25, 60 and 100 μm. The apertures were 18 arcsec for the three shortest wavelengths, 52 arcsec for 25 μm and 120 arcsec for the two longest wavelengths. The on-target photometric measurement was done with the same filter, aperture and integration time setup. The 150 and 200 μm maps were made with the 2×2 array in 2×2 spacecraft raster mode with steps of one pixel. This resulted in 3×3 images with 92 arc second pixels at 150 and 200 μm. The on-target pointings were centred on $\alpha_{\rm J2000} = 05$:04:30.0 and $\delta_{\rm J2000} = -03$:47:14.2 while the background measurement was at $\alpha_{\rm J2000} = 05$:04:30.0 and $\delta_{\rm J2000} = -03$:49:14.2.

The data were reduced with PIA 7.3.1 (Gabriel et al. 1997). In the reductions we followed the standard off-line processing steps with the following exceptions. For the 3.6–100 μm photometry we sub-divided the ramps into 4 parts in order to allow a better treatment of measurements where the response was drifting during the integration. For the spectrophotometry, we used so-called dynamic calibration where every wavelength is calibrated individually against a standard star which has its flux at the corresponding wavelength close to that of UX Ori. In all cases, the statistical errors are much less than the quoted calibration accuracies between 10 and 20 % which are listed in Table 3.

The photometric measurements at three wavelengths, 3.6, 12 and 25 μm have specific problems causing errors larger than the quoted 30 %. The 3.6 μm on-target measurement has more than a factor of two less power than in the calibration measurement for it. This is qualitatively understood as being due to non-linear behaviour, but cannot be quantified at this stage. The 12 and 25 μm measurements suffer from detector drifts and we cannot

Table 3. ISOPHOT photometry

λ [μm]	Flux [Jy]	Error
7.3	1.16	$\pm$0.12
60	2.15	$\pm$0.43
100	2.70	upper limit
150	0.65	$\pm$0.53
200	0.64	$\pm$0.27

be sure that a stable state had been reached in 32 s. We will not use these measurements in the following.

The spectrophotometric observation was not accompanied with an off-target measurement for a background estimate. We used the photometric background measurement assuming a featureless smooth continuum through the photometric points. This assumption is likely to be valid as the background is dominated by the zodiacal dust emission. The different apertures of the spectrophotometric and off-target photometric measurements were taken into account.

The background subtracted photometry of UX Ori is presented in Table 3. The 100 μm ISO measurement should be considered as an upper limit because the HIRAS map (Sect. 2.2) shows that extended emission dominates over any possible point source contribution at the chosen 2 arcmin diameter aperture.

The 150 and 200 μm maps both show the same kind of pattern. The centre pixel, corresponding to the position of UX Ori, has a higher value than any of the surrounding pixels. The maps are consistent with the background structure observed at the 100 μm HIRAS image (Fig. 2). Of the corner pixels the highest values are at NE and SW corresponding to the ridge between the clumps seen at 100 μm. We assume that the NE and SW corners give a better estimate of the background at the position of UX Ori than any of the lower surrounding pixels. With this background estimate we deduce 0.65 ± 0.53 and 0.64 ± 0.27 Jy at 150 and 200 μm respectively. The error estimates are based on the fluctuation observed at the pixel corresponding to the position of UX Ori at each of the four different raster points.

The mid-infrared spectrum of UX Ori shows a smooth flat continuum with the silicate feature in emission. The ISO data is consistent with earlier ground-based 10 μm spectroscopy (Reimann et al. 1997).

2.4. ISO-SWS

The SWS observation of UX Ori was obtained in an earlier revolution about 20 h before the photometry was done. The SWS measurement was part of a larger programme aimed at detecting H_2 in disks around young stars (Thi et al. 1999). The observation was done by scanning a small wavelength range around 7.0, 9.7, 17.0 and 28.2 μm. This configuration gave serendipitously also a measurement at 3.4 μm. The observation was centred on α_{J2000} =05:04:30.0 and $\delta_{J2000} = -$03:47:14.3. The data reduction is described in Thi et al., in preparation. The data were used to evaluate the continuum emission from UX Ori at the observed wavelengths. In order to estimate the background flux level of the continuum in the spectroscopic measurements, we scaled the photometric off-target measurements (Sect. 2.3) to the nominal SWS aperture sizes used in this observation. This is possible because the SWS measurements were done within one day of the ISOPHOT measurements with a solar aspect angle change of less than a degree between the observations resulting in equal zodiacal contribution. The background contribution is about 20% of the observed flux at 17.0 μm, and much less at the other wavelengths. The SWS fluxes are presented in Table 4.

2.5. The UX Ori SED

The spectral energy distribution (SED) of UX Ori of the whole wavelength range from 0.33 μm to 2.6 mm is shown in Fig. 3. We have complemented the data discussed above with three sets of photometric observations in the visual and near-IR obtained when the star was at its maximum brightness (Shevchenko et al. 1993; Kilkenny et al. 1985; Tjin A Djie et al. 1984).

The agreement between different observations is remarkably good. In particular, the PHOT-S fluxes agree very well with the SWS points at 3.4, 7 and 9.7 μm and with the ground-based photometry. Also, the IRAS broad-band flux centred at 25 μm is very close to the monocromatic flux measured by SWS at 28.2 μm.

At 1.3 mm, there is a single-dish measurement of 23$\pm$2 mJy, obtained with the IRAM 30m telescope (Natta et al. 1997), also shown in Fig. 3. The beam size was $11''$. This measure is, within the calibration uncertainties, roughly consistent with the interferometric flux reported above. There is no compelling evidence of extended millimetric emission associated with UX Ori on scales of about $10''$.

3. Evidence for a circumstellar disk around UX Ori

The detection of compact emission (radius $\lesssim 0.25''$ or $\lesssim$105 AU at D=430 pc) at 1.2 and 2.6 mm with the PdB interferometer provides strong evidence for the existence of a circumstellar disk around UX Ori. The argument, which is a classical one (see for example Beckwith et al. 1990) goes as follows. Let as assume that the emission comes from a spherical shell of dust of radius $\sim$ 100 AU around the star. We can evaluate its mass from the expression:

$$M_{dust} \sim 4 \times 10^{-5} \mathrm{M}_\odot \left(\frac{T}{15\mathrm{K}}\right)^{-1} \times \left(\frac{D}{430\mathrm{pc}}\right)^2 F_{1.2\,mm}(\mathrm{mJy}) \quad (1)$$

where we have assumed that the emission is optically thin and $\kappa_{1.2\,mm} = 1$ cm^2 g^{-1} of dust (Ossenkopf & Henning 1994). For $T = 90$ K (which is approximately the dust temperature at a distance of 100 AU from UX Ori; see Appendix B), we obtain $M_{dust} \sim 10^{-4}$ M$_\odot$. This, if distributed uniformly, corresponds to a visual extinction of about 850 mag, compared with the $\sim$ 0.3–0.5 mag one observes toward UX Ori. Hence, the circumstellar dust must have a highly non-spherically symmetric

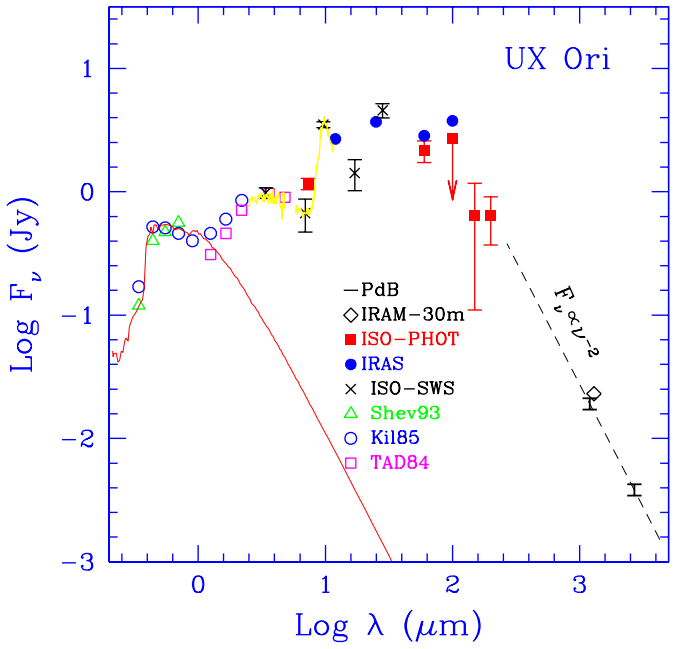

Fig. 3. Observed fluxes as function of wavelength. The symbols are described in the figure and have the following meaning: vertical bars are the Plateau de Bure observations, the open diamond is the 30m point (Natta et al. 1997); filled squares are the PHOT-S ISO observations; filled circles the four IRAS points; crosses the narrow-band continuum SWS fluxes; open squares refer to the near-infrared photometry of Tjin A Djie et al. (1984); open triangles from Shevchenko et al. (1993); open circles from Kilkenny et al. (1985). The thin solid line shows the stellar flux (Kurucz 1979) for the parameters given in Table 1.

Table 4. SWS Observations

λ (μm)	Flux (Jy)
3.4	1.0 ±0.1
7.0	0.7 ±0.2
9.7	3.5 ±0.2
17.0	1.4 ±0.4
28.2	4.6 ±0.6

distribution in order to allow the line of sight to the star to be unobstructed. It is reasonable to suppose that the dust is in a circumstellar disk.

We will discuss now the properties of such a disk. Disk models can have many different "flavors": disks can be flat, warped or flared, optically thick or thin; disk grains can be as small as in the interstellar medium or much larger. Disks can be rich or poor in gas. The word disk is often used in a very loose way, just to indicate a flattened distribution of matter around the star. Moreover, even if the observed millimeter emission is dominated by the disk, at shorter wavelengths we may observe radiation coming from other components of the circumstellar environment. Several authors have inferred from the SED the existence of spherical envelopes surrounding HAe/Be stars (Berrilli et al. 1992; Miroshnichenko et al. 1997; Pezzuto et al. 1998). In fact, the parameter space is huge and the distribution of gas and dust cannot be inferred from the SED alone.

Here we will follow a different approach. We start by examining the simplest disk models, similar to those which have been successfully proposed for TTS (black-body disks) and we will see if they can reproduce the interferometric millimeter observations under the constraint that the UX Ori system is seen close to edge-on (Sect. 3.1). As we will show, any such black-body disk model fails to account for the observed mid and near-infrared fluxes. However, models including the emission of the disk atmosphere, formed by the stellar radiation impinging on the disk surface, explain well the mid-IR emission (Sect. 3.2). We will then comment on possible origins for the near-IR flux (Sect. 3.3). In this way, we hope to obtain the "simplest" model of the UX Ori environment. Although we do not claim that our models are unique, we think they provide a useful starting point when discussing the complex properties of UXORs in general. A summary of the equations that describe the structure of our disk models and their emission is given in Appendix B.

3.1. Disk properties from millimeter observations

A first estimate of the properties of the UX Ori disk can be obtained from the observed millimeter fluxes. In the range 1.2–2.6 mm, the dependence of the flux on λ is close to that expected for a black body, with a spectral index $\alpha_{mm} = 2.1 \pm 0.2$.

A first approach to explaining this behaviour is to assume that the disk is optically thick at these wavelengths. We can make a rough estimate of the mass of such a disk (M_D^{thick}) requiring that the optical depth $\tau_{2.6\,mm} \sim \kappa_{2.6\,mm}\Sigma/\cos\theta \sim 1$ at the disk outer radius R_D. To estimate $\tau_{2.6\,mm}$, we describe the surface density as a power-law function of radius with exponent p. We can then write:

$$M_D^{thick} \sim 2\pi \frac{\tau_{2.6\,mm}}{\kappa_{2.6\,mm}} \frac{1}{2-p} \cos\theta\, R_D^2$$
$$\sim 0.73\,\mathrm{M}_\odot \cos\theta \left(\frac{R_D}{50\mathrm{AU}}\right)^2 \quad (2)$$

where θ is the viewing angle ($\theta = 90\,\mathrm{deg}$ for an edge-on disk) and we have assumed p=1.5, and dust opacity $\kappa \propto \lambda^{-\beta}$ with $\beta = 1$ and $\kappa_{1.2\,mm} = 0.01\,\mathrm{cm^2\,g^{-1}}$ (gas-to-dust ratio 100). The thick disk hypothesis requires a rather massive disk ($M_D^{thick} \sim 0.25$–$0.13(R_D/50\mathrm{AU})^2\,\mathrm{M}_\odot$) even for the large inclination of UX Ori ($\theta \sim 70$–$80\,\mathrm{deg}$).

We have computed the SED predicted by models of flat (i.e., geometrically thin) disks and of flared disks, assumed in hydrostatic equilibrium in the vertical direction (see Appendix B). For $M_D \gtrsim M_D^{thick}$ the flux at any given wavelength depends only on R_D and θ; more precisely, F_ν increases as R_D increases and decreases as the viewing angle θ increases. Table 5 provides a summary of the values of R_D and θ and of the minimum M_D of models that fit the 1.2 and 2.6 mm fluxes. Note that an upper limit $R_D \sim$100 AU is set by the Plateau de Bure observations; the smallest R_D corresponds to $\theta = 0$. Flat disks require lower values of θ and higher masses than flared disks. Fig. 4 shows the SED predicted by models with R_D=50 AU. Flat disks reproduce

Table 5. Disks Fitting the Millimeter Fluxes

R_D (AU)	θ (deg)	M_D ($M_\odot$)	Geometry
100	63	0.32	flat
50	46	0.28	flat
33	0	0.45	flat
100	86	0.12	flared
50	83	0.11	flared
30	74	0.08	flared
13	0	0.07	flared
100	any	0.12	flat,"pebble"
50	any	0.25	flat,"pebble"

the mm fluxes when seen at $\theta \sim 46$ deg, flared disk models for $\theta \sim 83$ deg. This high inclination agrees much better with the values derived from the behaviour of UX Ori in deep minima; this is a strong reason in favour of flared disks. The minimum disk mass required (for $R_D = 50$ AU) is $\sim 0.1\,M_\odot$.

A different family of disk models exists which can also give $\alpha_{mm} \sim 2$. These are disks, optically thin at millimeter wavelengths, where the dust opacity is independent of wavelength ($\beta = 0$). Large grain conglomerates with low filling factor tend to have slightly lower values of β at long wavelengths than compact grains (Pollack et al. 1994; Krügel & Siebenmorgen 1994; Ossenkopf & Henning 1994; Henning & Stognienko 1996). However, no realistic models (i.e., ruling out those that assume homogeneous conglomeration; Henning & Stognienko 1996) predict $\beta \sim 0$, unless the grains become very large (size $\gg \lambda$). In this case, it is likely that compaction of the grain components will occur, and the resulting cross section will resemble that of compact grains of similar size. From the results of Miyake & Nakagawa (1993) we estimate that grains of about 10 cm radius ("pebbles") have $\beta \sim 0$ at millimeter wavelengths; their opacity is $\sim 7 \times 10^{-4}$ cm^2 g^{-1} of gas at all wavelengths $\lesssim$1 cm; at 1.2 mm this is about 14 times lower than the value 0.01 cm^2 g^{-1} usually assumed to model pre-main–sequence disks. Fig. 4 shows (dot-dashed line) the SED of a disk made of 10 cm radius grains. The mass required to reproduce the observed millimeter fluxes is $\sim 0.25\,M_\odot$(R_D=50 AU), independently of the disk inclination. The emission is optically thin at all wavelengths longer than about 10 μm. Note that small "pebble" disks ($R_D \lesssim 30$ AU) are too weak at mm wavelengths. We have assumed a flat disk, since grain growth to such large sizes is likely restricted to the disk midplane.

The surface density profile adopted in computing the "pebble" disk models (p=1.5) has been derived empirically by Hayashi (1981) for the early solar nebula, and is commonly used in computing power-law disk models (see, for example, Beckwith et al. 1990). Recent observational results from millimeter interferometry and optical imaging with HST of disks around T Tauri stars suggest in some cases a flatter surface density profile, at least for the outer disk (see Wilner & Lay 2000). We have computed models with p=1, and found that the conclusions reached in this paper do not change significantly. The only disk parameter that varies is the disk mass required to fit the data, which is lower for p=1 by about a factor of 2.

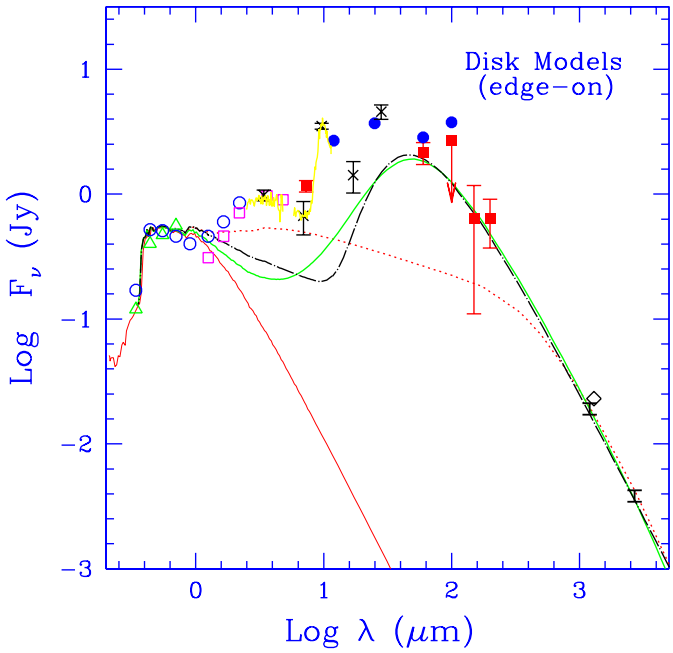

Fig. 4. Predicted SED of various disk models that fit the 1.2 and 2.6 mm interferometric fluxes. All models have R_D=50 AU. The dotted line refers to a flat disk of mass $M_D = 0.28\,M_\odot$, inner radius $R_0 = 2.3$ $R_\star$, seen at an inclination angle $\theta = 46$ deg. The solid line is a flared disk of mass $M_D = 0.11\,M_\odot$, R_0=1.4 $R_\star$, inclination angle 83 deg. In these optically thick disks, the SED does not depend on the surface density profile. The dot-dashed line shows the SED of a disk made of very large grains (radius$\sim$10 cm) with $\theta = 74$ deg, surface density $\propto R^{-1.5}$, mass is $M_D \sim 0.25\,M_\odot$. In this case, the flux at $\lambda \gtrsim 10$ μm does not depend much on θ. The thin solid line shows the observed stellar flux; the stellar parameters are given in Table 1. The lines plot the sum of the stellar + disk emission. The observed points are as in Fig. 3.

3.2. *The emission in the mid-infrared*

Both flat and flared disk models shown in Fig. 4 fail to reproduce the observed fluxes at wavelengths shorter than about 50 μm. In the mid-infrared, the observed spectrum, dominated by the strong emission feature at 10 μm, is immediately reminiscent of the optically thin emission of relatively hot dust. A natural (but not unique; see, for example, the case of GW Ori; Mathieu et al. 1995) location for this dust is in a disk atmosphere, as defined by Calvet et al. (1991) and CG97. The advantage of these models is that they do not require any *ad-hoc* additional geometric component for the circumstellar dust, since the properties of the atmosphere depends only on the stellar parameters and on the disk structure.

We compute disk models which include the emission of the disk atmosphere following CG97. In their model, the stellar radiation penetrates the disk outer layers to an optical depth $\sim$1 along the disk plane. Dust in this outer region is superheated

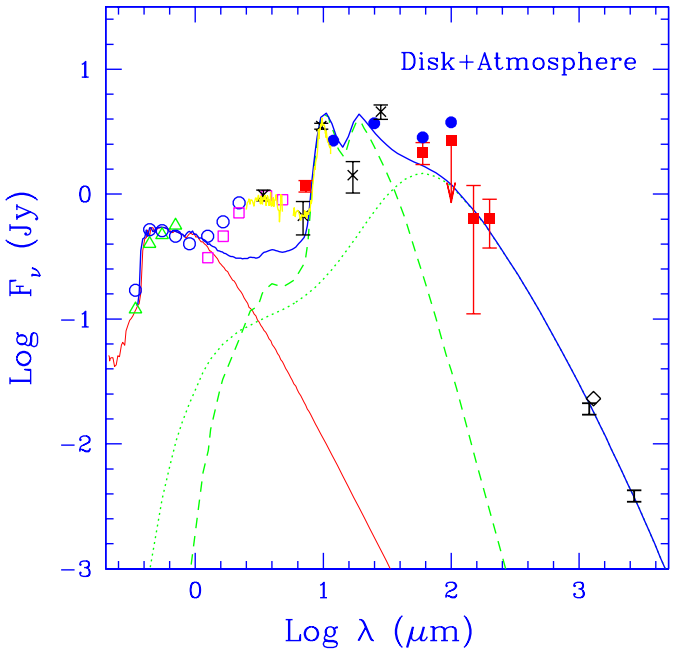

Fig. 5. SED of the flared disk+atmosphere model (solid line). The disk has the same parameters of the flared disk shown by the solid line in Fig. 4, with the exception of θ which is in this case $\sim 80\,\mathrm{deg}$ to compensate for the fact that the disk midplane is slightly cooler than in a "naked" disk (see Appendix B). The separate contribution of the disk midplane and of the atmosphere are shown by the dotted and dashed lines, respectively. Observed points as in Fig. 3.

(with respect to the dust in the disk midplane) to temperatures typical of optically thin dust. The emission of the superheated layer (i.e., the disk atmosphere), rather than direct stellar light, heats the disk midplane. The expressions to compute the disk temperature are given in CG97 and summarized in Appendix B. The models in Fig. 5 have been computed for a flared disk; the dust opacity in the atmosphere is that of 1μm Draine & Lee (1984) silicates; the disk parameters, including dust properties in the disk, are the same as in the flared disk model displayed in Fig. 4. Note that the dust in the disk atmosphere can be different, less evolved, than that in the disk midplane.

The emission of the superheated layer peaks in the wavelength region between ∼10 and ∼40 μm for disks with $R_D \gtrsim 30$ AU (it is narrower if R_D is smaller). Outside this wavelength range, the SED is dominated by the emission of the disk midplane. These models reproduce well the observed strength of the 10 μm silicate emission and the excess continuum flux (with respect to the emission of the optically thick disk) in the mid-infrared. The intensity and qualitative shape of the atmospheric emission depend on the stellar radiation field, on the disk flaring, and on the ratio of the dust opacity at the peak of the stellar radiation (about 4600 Å in the case of UX Ori) to that in the mid-infrared. The details of the emission depend strongly on the adopted dust properties. For example, the fit to the observed shape of the 10 μm silicate feature could be improved assuming 1 μm size glassy pyroxene (Reimann et al. 1997), rather than standard interstellar silicates. However, the analysis of the dust properties in UX Ori is hindered by the lack of a high-resolution mid-infrared spectrum, such as those obtained by SWS for other, brighter HAe/Be stars, and will not be discussed further in this paper.

In computing these models, we have assumed that the emission of the optically thick disk midplane varies as $\cos\theta$, while the emission of the superheated layer is independent of θ. In a recent paper, Chiang & Goldreich (1999) discuss the effects of the inclination on their models. From their results, we can see that the prescription we have adopted holds as long as $\theta < \theta_0$, where θ_0 depends on the amount of disk flaring at R_D; for the UX Ori disk it is $\theta_0 \sim 70\,\mathrm{deg}$ at R_D=50 AU, and $\theta_0 \sim 73\,\mathrm{deg}$ at R_D=30 AU. For $\theta \gg \theta_0$, the intervening outer disk occults the short-wavelength emission of the inner disk and of the star itself. The limiting value θ_0 is close to the required inclination for R_D=30 AU, and somewhat smaller for R_D=50 AU. It may be possible to use this information to further constrain R_D. This, however, requires more detailed models, where the extinction due to the intercepted outer disk layers is carefully taken into accout; they are beyond the scope of this paper.

The emission of the atmosphere of a flat disk is much weaker than that shown in Fig. 5, since its vertical extent is much smaller, and cannot account for the observed mid-infrared fluxes. This is a second, strong argument in support of flared disk models. It suggests that most of the disk mass is in the gas. The amount of flaring in a disk in hydrostatic equilibrium is inversely proportional to the half power of the mean molecular weight (see Appendix B); if dust dominates the disk mass, the flaring will be negligible. This argument also suggests that the UX Ori disk cannot be formed only by very large grains. We will come back to this point in the following section.

3.3. The emission in the near-infrared

The main failure of all the disk models with large inclination with respect to the line of sight is their inability to account for the strong near-infrared emission in UX Ori, which amounts to about 4.9 $L_\odot$ (between 2.2 and 7.2 μm). This value is very close to the luminosity over the same wavelength interval of disks seen face-on, which is about 5 $L_\odot$ in all our disk models (flat, flared and "pebble" disks). Let us release for a moment the condition of large θ, derived from the photometric and polarimetric variability. The emission of mm-thick disks scales at all wavelengths as $\cos\theta$. They cannot account simultaneously for the near-IR and millimeter fluxes, since face-on disks predict millimeter fluxes by far higher than observed (unless they are very small, in which case their atmospheric emission is negligible). "Pebble" disks are optically thin at mm wavelengths, but thick in the near-infrared. A "pebble" disk seen face-on provides the best fit to both near-infrared and millimeter fluxes (Fig. 6). Note, however, that there is still observed excess emission around 5 μm. We will come back to this point in the following section.

It is likely that a contribution at near-infrared wavelengths comes from scattered light, as the radiation emitted by the inner disk (the stellar contribution is negligible) hits the outer surface of the flared disk and is scattered toward the observer. Such

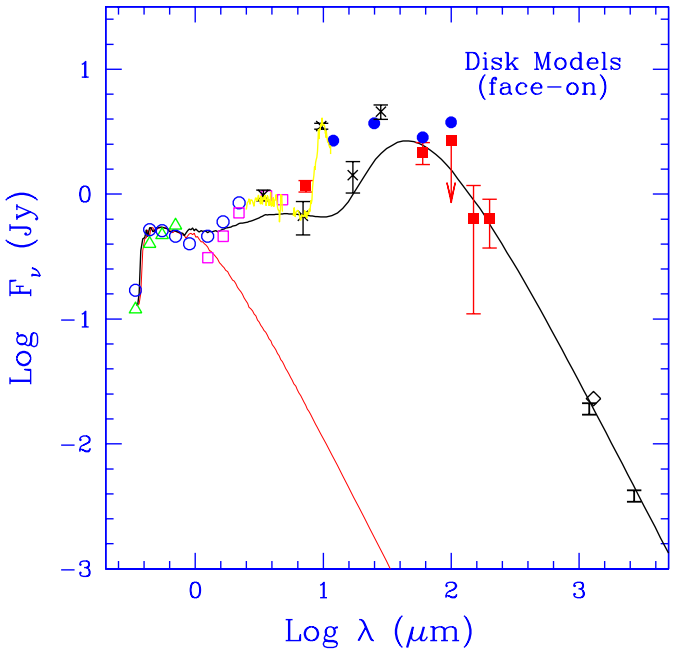

Fig. 6. The solid line shows the SED of a disk made of very large grains (radius$\sim$10 cm) seen face-on ($\theta = 0\,\mathrm{deg}$). The disk has mass $M_D = 0.23\,\mathrm{M}_\odot$, inner radius $R_0 = 2.7\,\mathrm{R}_\star$, outer radius $R_D = 50$ AU, surface density $\propto R^{-1.5}$. The line plots the sum of the stellar and disk emission. Observed points as in Fig. 3.

models provide the most straightforward interpretation of the resolved images of disks obtained for several objects with HST in the visual and in the near-infrared (see McCaughrean et al. 2000 and references therein).

However, simple energetic considerations suggest that scattered light cannot account for all the observed flux. If we consider the most favorable case of a flared disk, its opening angle is about 20 deg at $R_D = 50$ AU, so that the outer disk can intercept at most 6% of the inner disk emission or 0.3 $\mathrm{L}_\odot$, a value by far too low when compared to the observed luminosity in this wavelength range. In fact, the TTS with resolved disks in the HST sample tend to be very weak near-infrared sources (Stapelfeldt et al. 1997; Stapelfeldt & Moneti 1999). We will briefly discuss alternative possibilities in Sect. 4.

3.4. Scattered light in the visual

An important point we want to stress is that scattering of the stellar radiation at visual wavelengths by the grains in the optically-thin disk atmosphere is likely to be a significant fraction of the observed light when the star is occulted by an intervening clump. The mm-thick flared disks discussed in Sect. 3.1 intercepts about 30% of $\mathrm{L}_\star$; assuming an albedo of 0.5, and that, as for the atmospheric emission, all the light scattered by one side of the disk reaches the observer, we obtain about 3.5 $\mathrm{L}_\odot$ in scattered light, i.e., $\sim$10% of the flux received by the observer. However, in a deep minimum, when UX Ori fades by about 2.5 mag, the contribution of this disk-scattered light dominates the observed flux.

We suggest here that the flattened cloud of small particles, which has been used to explain the blueing of the stellar colors and the increase in the polarization of the stellar light during minima (Voshchinnikov 1998; Friedemann et al. 1994), is in fact the optically thin atmosphere of an optically thick disk. If confirmed by detailed calculations, this could provide an important simplification in the description of the circumstellar matter associated to UX Ori.

4. Discussion

The presence of a circumstellar dusty disk in UX Ori is well established by the millimeter interferometric observations. They can be fit by two families of disk models, one of disks with standard grain properties, massive enough to be optically thick at millimeter wavelengths (mm-thick disks), and one of disks (optically thin in the millimeter) where most solids have grown to large sizes (about 10 cm), so that their opacity does not depend on wavelength ("pebble" disks). In the previous section, we have discussed the model-predicted SED for both kind of models, making use of the additional constraint, derived from the analysis of simultaneous photometric and polarimetric observations in the visual, that the disk must be seen almost edge-on.

4.1. "Pebble" disks

"Pebble" disks, where most of the dust in the disk midplane has accreted into very large grains ($\sim$10 cm), requires a large disk mass (~ 0.1–$0.25\,\mathrm{M}_\odot$) and the rather high ratio of the disk-to-star mass of ~ 0.04–0.1. Although we do not know the present gas-to-dust mass ratio (all the disk masses quoted so far have been computed assuming a 100:1 ratio), our estimate of M_D should, in any case, reflect the disk mass in its early stages, before gas dissipation occurs. In fact, we have indirect evidence (from the strength of the mid-IR flux; see Sect. 3.2) that most of the UX Ori disk mass is still contributed by gas. Very likely, small grains are still mixed with the gas, at least above and below the disk midplane, where grain growth to cm sizes could have occurred. We can estimate an upper limit to the mass of small grains considering that, in order to keep $\alpha_{mm} \sim 2$, the contribution of the small grains to the mm opacity must be negligible, let's say 10% of that of the 10 cm-radius grains. The corresponding limit to the mass of small grains is about 7×10^{-3} that of large grains, i.e., $\sim 0.002\,\mathrm{M}_\odot$. We cannot predict, using our simple models, the SED of disks with a vertical stratification of grain sizes. In particular, we cannot estimate the extent and emission of a disk atmosphere in the simple way described in Appendix B. The small grains, if they have a broader vertical distribution than the large ones, intercept a significant fraction of the stellar radiation, so that it is possible that the atmospheric structure is not changed much. Models more complex than those we have used are clearly required to further discuss this hypothesis. However, it seems clear that disks made only of very large grains cannot explain the UX Ori SED. Rather, a mixture of

large grains, smaller grains and gas are required. Such disks will have to be rather massive.

4.2. MM-thick disks

Flared, mm-thick disks seen almost edge-on are successful in accounting for the observed fluxes at all wavelengths longer than ~ 8 μm. Also in this case, as for "pebble" disks, the UX Ori disk is rather massive ($\gtrsim 0.1\,M_\odot$).

Few stars in the sample studied by Natta et al. (2000) have $M_D \gtrsim 0.1\,M_\odot$, and they are all much more embedded than UX Ori.

4.3. The near-IR puzzle

The only serious shortcoming of our disk models is their failure to account for the near-infrared emission of UX Ori (see Figs. 4 and 5), if we accept the constraint that the disks are seen almost edge-on.

There are a number of effects that can possibly enhance the near-IR emission of the UX Ori disk. First of all, our disk models have a very simple geometry. It is possible that the inner disk is more extended in the vertical direction than we have assumed (see, for example, Bell et al. 1997). Such disks intercept and re-emit in the near-IR a larger fraction of the stellar radiation. Also, disks can be warped, so that the viewing angle θ depends on R. β Pic, for example, has a strongly warped disk (Lagage & Pantin 1994; Heap et al. 1999); Armitage & Pringle (1997) discuss warping induced by radiation pressure in pre-main–sequence disks. All our disk models neglect heating due to viscous dissipation of accretion luminosity. In a flared disk, viscosity can dominate the heating of the inner disk, and be negligible in the outer disk. However, we estimate that an accretion rate $\dot{M}_{ac} \sim 10^{-6}\,M_\odot\,\mathrm{yr}^{-1}$, corresponding to the very high accretion luminosity of about 10 $L_\odot$($\sim 0.25\,L_\star$; there is no evidence of significant accretion in the spectrum of UX Ori) will only increase the near-IR emission by a factor of 2.

Finally, we have examined the possibility that the near-infrared emission finds a natural explanation within the models which explain the visual variability of UX Ori as due to clumps of dust occulting the star. Such clumps intercept a fraction of the stellar light and, when near the star, re-emit it in the near-infrared. If the clumps are orbiting the star at a distance of about 10 AU (as derived from the observed duration of the deep minima, which is of order of days; Voshchinnikov & Grinin 1991), they will be too cold ($\lesssim$300 K) to emit significantly in the near-IR. However, let us assume that the clumps are related to a family of massive solid bodies (protocomets?) that approach the star on highly elongated orbits; an occulting clump is then just the coma of some of such bodies. As they come closer to the star, they get hotter and emit in the near-IR, until all the grains are evaporated. A correlation between the near-infrared emission and the minima of the star has been observed in two UXORs (Sitko et al. 1994; Hutchinson et al. 1994). There is also some hint of variability in the IRAS measurements at 12 and 25 μm of two UXOR stars, AB Aur and WW Vul, possibly associated to cometary clumps in eccentric orbits (Prusti & Mitskevich 1994). The possible relation between the near-infrared emission and the clumps of dust responsible for the sporadic occultation of the star is exciting and certainly deserves further investigations. At present, however, it is not supported by any quantitative analysis.

The constraint of high-θ for the UX Ori disks derives from the "occultation" interpretation of the deep minima. As mentioned in the introduction, this appears to be, at the moment, the best explanation. However, it is not unique. For example, Herbst & Shevchenko (1999) suggest that UXOR phenomena may be related to variable accretion through a disk, as in FUORs. When the UXOR is at maximum, we do not observe the stellar photosphere but rather the emission of the inner disk; the deep minima would then corresponds to periods of lower accretion. The main objection to this idea, that has not been developed in any quantitative way, is the lack of similarity of the optical spectrum of UX Ori to the accretion-dominated FUORS. However, the failure of the edge-on disk models to account for the near-IR emission of UX Ori invites us to investigate the UXOR nature with open mind. We are intrigued by the fact that, as we have discussed, "pebble" disks seen face-on provide the best fit (although not a perfect one!) to the observed SED at all wavelengths, provided that they can keep a flared atmosphere of smaller grains.

4.4. Comparison with other stars

The picture we have been outlining for UX Ori is that of a disk of radius about 50–100 AU, very inclined with respect to the line of sight. The disk is rather massive ($\gtrsim 0.1\,M_\odot$). We cannot determine on the basis of the SED if grain growth to $\gtrsim$10 cm radius has occurred in the disk midplane or not. The disk emission dominates the observed flux at all wavelengths $\gtrsim$ 8–9μm, as emission of the thick disk midplane (at $\lambda \gtrsim 60$ μm) and of the optically thin disk atmosphere that enshrouds the disk (at 8–9 $\lesssim \lambda \lesssim 30$ μm). Grains in these outer layers are likely to scatter a significant fraction of the stellar radiation, which is seen in the visual when the direct stellar light is occulted. There is a significant near-IR excess, which is not accounted for by such simple disk models. Is this picture typical of UXORs, of Herbig Ae stars in general, or just of UX Ori? At present, not enough is known to answer this question. One needs accurately measured SED over the whole range of wavelengths, including information on the silicate features, interferometric millimeter data that can clarify the disk properties, and good information on the inclination from variability studies at optical frequencies. Although HAe/Be stars have been the subject of increasing attention in recent years, the information is still sparse.

Most of our results depend critically on the interferometric fluxes at 1.2 and 2.6 mm. The only other UXOR for which this information exists is CQ Tau, a UXOR of spectral type A8–F0 at distance of 100 pc, where Mannings & Sargent (1997, 1999) detected compact millimeter emission at 1.2 and 2.6 mm with the OVRO interferometer. The spectral index in CQ Tau is $\alpha_{mm} = 2.9 \pm 0.2$, entirely consistent with an optically thin

emission from grains with $\beta \sim 1$, typical of most pre-main–sequence disks (Beckwith et al. 1990). The disk mass determined by Natta et al. (2000), assuming optically thin emission at 1.2 mm, is 0.03 $M_\odot$. Thus, the CQ Tau disk does not have $\beta \sim 0$, and is less massive than that of UX Ori. However, CQ Tau is unresolved by OVRO in the mm-continuum, with a limit $R_D < 80$ AU. It seems that CQ Tau and UX Ori both have very small disks (in continuum emission). Is this typical of UXORs? A much larger sample is certainly needed.

5. Summary and conclusions

We have dicussed in this paper new observations of the star UX Ori obtained with the millimeter interferometer of Plateau de Bure and with ISO. UX Ori is the prototype of UXORs, a group of pre-main–sequence stars of intermediate mass which show large, irregular photometric variability (Herbst et al. 1994). UXORs have been indicated as possible precursors of β Pic-systems, and, as such, have attracted considerable attention in recent years (see, for example, Pérez & Grady 1997; Waters & Waelkens 1998 and references therein).

The interferometric observations at 1.2 and 2.6 mm show that UX Ori has a circumstellar disk, with outer radius $\lesssim$100 AU. The spectral index between these two wavelengths ($\alpha_{mm} = 2.1 \pm 0.2$) is consistent with the disk being optically thick at mm waveleghts. In this case, the disk is rather massive ($M_D \gtrsim 0.1\,M_\odot$). A self-consistent model of mm-thick disk, heated by stellar radiation, accounts well for the observed emission at all wavelengths longer than about 8μm, if we include the emission of the optically thin, superheated outer layers (the disk atmosphere; see CG97). We suggest that the grains in these outer layers can also account for the scattered light observed when the star is in a deep minimum. The observed α_{mm} is also consistent with emission from very large grains (radius $\gtrsim$10 cm). Also in this case $M_D \gtrsim 0.1\,M_\odot$. As in the case of mm-thick disks, most of the disk mass must be gaseous and a small, but not negligible dust mass must be in small grains.

The disk models fail to account for the rather strong emission observed in the near-IR (i.e., in the interval $\sim$ 2–7 μm) if we take into account the constraint, set by polarimetric and photometric visual variability, that the disk must be seen almost edge-on ($\theta \gtrsim 70$ deg; Voshchinnikov et al. 1988). We suggest a number of possible explanations, among them that this excess could be associated to the "clumps" that sporadically occult the star. The nature and origin of the clump system is not clear. If, as suggested in the case of β Pic, it is the young equivalent of the Oort cloud, then in UX Ori we have at the same time a "young", massive disk of small grains and gas and a component typical of later phases of the planet formation process. However, there are alternative explanations, where the near-infrared excess is due to changes in the disk structure with respect to our simple models. Let us also point out that the identification of the occulting clumps with "protocomets" is not the only possibility. "Clumps" could be density fluctuations in the disk vertical structure; this possibility should also be investigated further. Finally, alternative models for the UXOR activity, that do not constrain the angle of view, should be taken into consideration.

The UX Ori observations presented in this paper and their interpretation may offer a valuable guideline for the analysis of other UXORs. In particular, it is of great interest to find out which (if any) of the UX Ori properties we have identified are typical of UXORs and make them different from non-variable Herbig Ae stars. At present, as discussed in Sect. 5, the available data do not give any answer to this question. We expect, however, that this will change in the near future, as visual, infrared and millimeter data of more and carefully selected objects will become available.

Acknowledgements. This work was partly supported by ASI grant ARS-98-116 to the Osservatorio di Arcetri. V.P.G. was supported in part by RFFI grant 99-02-18520.

Appendix A: stellar parameters

The distance to UX Ori has been estimated by Warren & Hesser (1978) to be 430 pc. The spectral type A3 III (Timoshenko 1985) corresponds to an effective temperature $T_\star$=8600 K (Schmidt-Kaler 1982). We have fit a model stellar atmosphere with $T_\star$=8600 K and gravity Log g=3.8 (Kurucz 1979) to the photometric points in the bands U, B, V, R, I measured when the star was close to maximum light. We found good agreement for A_V=0.5 mag.

For $D = 430$ pc, the corresponding luminosity is 36 $L_\odot$. However, a circumstellar disk surrounding the star will intercept a fraction of its radiation and one must correct for that. The correction factor depends on the viewing agle θ and is of order of 1.5 for $\theta = 70$ deg if the disk extends to the stellar surface (Adams & Shu 1986); it is smaller if the disk has an inner hole. We find good agreement between model-predicted fluxes and observations for a correction factor 1.25; the resulting luminosity is then 48 $L_\odot$. With these values of $T_\star$ and $L_\star$, the location of UX Ori on the HR diagram corresponds to a mass of 2.5 $M_\odot$ and an age of 2×10^6 yr, when compared to the evolutionary tracks of Palla & Stahler (1993). Note that the uncertainty on $L_\star$ due to the uncertainty on the inclination and inner disk radius may affect somewhat the parameters of the best-fitting disk models derived in Sect. 3. However, none of the more general results of this paper is affected.

The inclination ($\theta \gtrsim 70$ deg; $\theta = 90$ deg for a edge-on disk) is determined by Voshchinnikov et al. (1988) from visual polarimetric observations as the star goes through a deep minimum.

Appendix B: disk models

Let us consider a disk with inner radius R_0, outer radius R_D. The disk is heated by a star of luminosity $L_\star$, temperature $T_\star$and radius $R_\star$. R is the distance from the star in the disk midplane and $x = R/R_\star$. At all radii, the disk is optically thick to the stellar radiation *and* to its own emission.

Under these assumptions, the temperature in the disk midplane (for $x \gg 1$) can be computed as:

$$T_D \sim \left(\frac{\alpha}{2}\right)^{1/4} x^{-1/2}\, T_\star \tag{B1}$$

where α is the flaring angle at x. In a geometrically flat disk, $\alpha \sim 0.4\, x^{-1}$ and the temperature has the well-known dependence (Adams & Shu 1986):

$$T_D = 0.68\, T_\star\, x^{-3/4} \tag{B2}$$

If the disk is in hydrostatic equilibrium between gravity and thermal pressure, it will be flared (Kenyon & Hartmann 1987). The flaring angle α is given by:

$$\alpha = 0.4\, x^{-1} \,+\, 1.1 \left(\frac{T_\star}{T_g}\right)^{4/7} x^{2/7} \tag{B3}$$

where (μ is the mean molecular weight):

$$T_g = \frac{GM_\star\, \mu}{KR_\star} \tag{B4}$$

In both cases (flat and flared disks), the flux received by an observer at distance D, who sees the disk with an inclination angle θ ($\theta = 90\,\mathrm{deg}$ for an edge-on disk) is:

$$F_\nu = \cos\theta\, \frac{1}{D^2} \int_{x_0}^{x_D} B_\nu(T_D)\, 2\pi\, x dx \tag{B5}$$

CG97 have pointed out that the stellar radiation does not reach the disk midplane, but is absorbed in an outer layer of optical depth $\tau = 1$ in the direction parallel to the the disk plane. The extension in the orthogonal direction is much smaller ($\tau_\perp \sim \tau\, \alpha \sim \alpha$). Grains in this layer (the superheated layer or disk atmosphere) have their temperature determined by the balance between their emission and the absorption of the stellar radiation attenuated only by geometrical dilution. Using the spherically symmetric radiation transfer code kindly made available to us by E. Krügel, we find that the temperature of silicates of $\sim 1\mu$m radius in the disk atmosphere T_a can be expressed as:

$$T_a = 0.76\, T_\star\, x^{-0.48} \tag{B6}$$

The dust in the optically thick underlying disk (the disk midplane) is heated by the emission of the outer layer, i.e., only indirectly by the stellar radiation. Its temperature has been computed by CG97 and, if the disk is thick at all wavelengths, it is:

$$T_D \sim \left(\frac{\alpha}{4}\right)^{1/4} x^{-1/2}\, T_\star \tag{B7}$$

The observed flux is the sum of the emission of the disk midplane, given by Eq. (B5) with T_D given by Eq. (B7), plus the emission of the optically thin disk atmosphere. This second term does not depend significantly on θ, as long as the line of sight does not intercept the disk outer region, i.e., as long as $\theta \lesssim H/R$ at R_D.

Note that if the disk is optically thick at all wavelengths, F_ν does not depend on the surface density. However, the disk mass does. If the surface density can be described by a power-law ($\Sigma = \Sigma_0\, x^{-p}$), it is:

$$M_D = 2\pi\, R_0^2\, \Sigma_0\, \frac{1}{2-p}\, (x_D^{2-p} - 1) \tag{B8}$$

"Pebble" disks have an opacity $\kappa = \bar{\kappa}$ which is constant at all wavelengths. The disk is thick to the absorbed and emitted radiation up to radii of $\sim$12 AU (for $\bar{\kappa} = 7 \times 10^{-4}\,\mathrm{cm^2 g^{-1}}$) and T_D is given by Eq. (B1). At larger radii, it is optically thin to *both* emitted and absorbed radiation and it is:

$$T_D \sim 0.7\, T_\star\, x^{-1/2} \tag{B9}$$

The observed flux is given by:

$$F_\nu = \cos\theta\, \frac{1}{D^2} \int_{x_0}^{x_D} \pi B_\nu(T_D)\, (1 - e^{-\bar{\tau}})\, 2\pi\, x dx \tag{B10}$$

where

$$\bar{\tau} = \frac{1}{\cos\theta}\, \Sigma\, \bar{\kappa} \tag{B11}$$

References

Adams F.C., Shu F.H., 1986, ApJ 308, 836
Armitage P.J., Pringle J.E., 1997, ApJ 488, L47
Beckwith S.V.W., Sargent A.I., Chini R.S., Güsten R., 1990, AJ 99, 924
Bell K.R., Cassen P.M., Klahr H.H., Henning Th., 1997, ApJ 486, 372
Berrilli F., Corciulo G., Ingrosso G., et al., 1992, ApJ 398, 254
Bibo E.A., Thé P.S., 1990, A&A 236, 155
Bibo E.A., Thé P.S., 1991, A&AS 89, 319
Bontekoe Tj.R., Koper E., Kester D.J., 1994, A&A 284, 1037
Calvet N., Patino A., Magris G.C., D'Alessio P., 1991, ApJ 380, 617
Chiang E.I., Goldreich P., 1997, ApJ 490, 368
Chiang E.I., Goldreich P., 1999, ApJ 519, 279
D'Alessio P., Cantó J., Calvet N., Lizano S., 1998, ApJ 500, 411
Draine B.T., Lee H.M., 1984, ApJ 285, 89
Friedemann C., Reimann H.G., Gürtler J., 1994, Ap&SS 212, 221
Gabriel C., Acosta-Pulido J., Heinrichsen I., Morris H., Tai W.-M., 1997, PASPC 125, 108
Grady C.A., Sitko M.L., Russell R.W., et al., 2000, In: Mannings V., Boss A.P., Russell S.R. (eds.) Protostars and Planets IV, University of Arizona Press, Tucson, in press
Grinin V.P., 1988, Pis'ma v Astron. Zn. 14, 65
Grinin V.P., Thé P.S., De Winter D., et al., 1994, A&A 292, 165
Grinin V.P., Kiselev N.N., Minikhulov N.Kh., Chernova G.P., Voshchinnikov N.V., 1991, Ap&SS 186, 283
Hayashi C., 1981, PThPS 70, 35
Heap S.R., Linder D.J., Lanz T.M., et al., 1999, ApJ, in press
Henning Th., Stognienko R., 1996, A&A 311, 291
Herbst W., Herbst D.K., Grossman E.J., Weinsyein D., 1994, AJ 108, 1906
Herbst W., Shevchenko V.S., 1999, AJ, in press
Hillenbrand L.A., Strom S.E., Vrba F.J., Keene J., 1992, ApJ 397, 613
Hutchinson M.G., Albinson J.S., Barrett P., et al., 1994, A&A 285, 883
Kenyon S.J., Hartmann L., 1987, ApJ 322, 293
Kilkenny D., Whittet D.C., Davies J.K., et al., 1985, SAAOC 9, 55
Krügel E., Siebenmorgen R., 1994, A&A 288, 929
Kurucz R.L., 1979, ApJS 40, 1
Lagage P.O., Pantin E., 1994, Nat 369, 628

Mannings V., Sargent A.I., 1997, ApJ 490, 792
Mannings V., Sargent A.I., 1999, ApJ, submitted
Mathieu R.D., Adams F.C., Fuller G.A., et al., 1995, AJ 109, 2655
McCaughrean M.J., Stapelfeldt K.R., Close L.M., 2000, In: Mannings V., Boss A.P., Russell S.R. (eds.) Protostars and Planets IV, University of Arizona Press, Tucson, in press
Meeus G., Waelkens C., Malfait K., 1998, A&A 329, 131
Miroshnichenko A., Ivezic Z., Elitzur M., 1997, ApJ 475, L41
Miyake K., Nakagawa Y.K., 1993, Icarus 80, 189
Natta A., Grinin V.P., Mannings V., Ungerechts H., 1997, ApJ 491, 885
Natta A., Grinin V.P., Mannings V., 2000, In: Mannings V., Boss A.P., Russell S.R. (eds.) Protostars and Planets IV, University of Arizona Press, Tucson, in press
Ossenkopf V., Henning Th., 1994, A&A 291, 943
Palla F., Stahler S.W., 1993, ApJ 418, 414
Pérez M.R., Grady C.A., 1997, Space Sci. Rev. 82, 407
Pezzuto S., Strafella S., Lorenzetti D., 1998, ApJ 485, 290
Pollack J.B., Hollenbach D., Beckwith S., et al., 1994, ApJ 421, 615
Prusti T., Mitskevitch A., 1994, In: Thé P.S., Pérez M., van den Heuvel P.J. (eds.) The Nature and Evolutionary Status of Herbig Ae/Be Stars. PASPC 62, 257
Reimann H.-G., Gürtler J., Friedemann C., Käufl H.U., 1997, A&A 326, 271
Schmidt-Kaler Th., 1982, In: Schaifers K., Voigt H.H. (eds.) Landolt-Börnstein, Numerical Data and Functional relationships in Science and Technology. Group VI, Astronomy, Astrophysics and Space Research Vol. 2b, Springer-Verlag, Berlin, p. 15
Shevchenko V.S., Grankin K.N., Ibragimov M.A., Mel'nikov S.Yu., Yakubov S.D., 1993, Ap&SS 202, 121
Sitko M.L., Halbedel E.M., Lawrence G.F., Smith J.A., Yanow K., 1994, ApJ 432, 753
Stapelfeldt K., Moneti A., 1999, In: Cox P., Kessler M.F. (eds.) The Universe as seen by ISO, in press
Stapelfeldt K., Burrows C.J., Krist J.E., WFPC2 Science Team, 1997, In: Reipurth B., Bertout C. (eds.) Herbig-Haro Flows and the Birth of Low Mass Stars. IAU Symp. 182, Kluwer, Dordrecht, p. 355
Timoshenko L.V., 1985, Astrofizika 22, 51
Thi W.F., van Dishoek E.F., Blake G.A., et al., 1999, In: Cox P., Kessler M.F. (eds.) The Universe as seen by ISO, in press
Tjin A Djie H.R.E., Remijn L., Thé P.S., 1984, A&A 134, 273
Voshchinnikov N.V., 1998, Astron.Rept. 42, 54
Voshchinnikov N.V., Grinin V.P., 1991, Astrofizika 34, 181
Voshchinnikov N.V., Grinin V.P., Kiselev N.N., Minikhulov N.Kh., 1988, Astrofizika 28, 182
Warren W.H. Jr., Hesser J.E., 1978, ApJS 36, 497
Waters L.B.F.M., Waelkens C., 1998, ARA&A 36, 233
Wilner D.J., Lay O.P., 2000, In: Mannings V., Boss A.P., Russell S.R. (eds.) Protostars and Planets IV, University of Arizona Press, Tucson, in press